Theoretical Population Biology **53**, 216–235 (1998)
Article No. TP971360

Evolutionary Stable Strategies and Trade-Offs in Generalized Beverton and Holt Growth Models

Schalk W. Schoombie

Department of Mathematics and Applied Mathematics, University of the Orange Free State, P.O. Box 339, Bloemfontein 9300, South Africa

and

Wayne M. Getz

Department of Environmental Sciences, Policy, and Management, University of California at Berkeley, Berkeley 94720-3112, California

Received February 21, 1997

A generalized Beverton–Holt model is considered in which a parameter γ characterizes the onset of density dependence. An evolutionary stable strategy analysis of this parameter, reported in Getz (1996), is developed further here, using invasion exponents and the strategy dynamics of Vincent *et al*. (1993). The parameter γ is also allowed to be density dependent, and it is shown that the most successful strategies of this type are those for which γ is large for low densities and close to its minimum for high densities. A biological interpretation is given in the context of mobile females depositing their relatively sessile young on patches of resource, namely, females should overdisperse their young on resources when adult densities are high and underdisperse them when these densities are low. Finally the per capita growth rate parameter is also allowed to depend on γ. It is shown that this dependence provides a mechanism by which periodic or chaotic attractor dynamics could evolve towards equilibrium attractor dynamics.

1. INTRODUCTION

The dynamic behavior of discrete scalar population models can be complex for parameter values that admit oscillatory (cyclic and chaotic) solutions. In particular, the generalized Beverton–Holt model (density-dependence has an inverse sigmoidal form)

$$x_{t+1} = \frac{rx_t}{1+(x_t/K)^{\gamma}}, \quad \gamma > 1, \tag{1}$$

recently explored by one of us (Getz, 1996), admits chaotic solutions when the density dependent "abruptness" parameter γ is sufficiently large in relation to the per capita growth rate parameter r: i.e., oscillatory solutions occur when $\gamma > 2r/(r-1)$. The generalized Beverton–Holt model (1), although not as widely used as the logistic or Ricker models, has been applied to several population studies (Maynard Smith and Slatkin, 1973; Maynard Smith, 1973; Getz and Kaitala, 1989; Kaitala *et. al.*, 1989, 1993; Shepherd, 1982; Doebeli, 1995; Getz, 1996), and has been shown by Bellows (1981) to fit insect

0040-5809/98 $25.00

population data better than other elementary models. From a biological point of view, the parameter γ should be constrained to ensure that the derivative of the function $f(x) = r/(1 + (x/K)^{\gamma})$ is zero at $x = 0$, or at least not equal to its most negative value, since the effects of density dependence should be minimal at the lowest densities (for more details see Getz, 1996). This is ensured by the constraint $\gamma > 1$. For $\gamma = 1$, df/dx takes on its most negative value at $x = 0$; but we still add the point, $\gamma = 1$, however, to close the interval, thereby ensuring the existence of evolutionary stable strategy (ESS) solutions when they would otherwise not be defined. For $0 \leqslant \gamma < 1$, df/dx is $-\infty$ at $x = 0$, which makes no biological sense, even if the problem is still well-posed from a mathematical point of view.

An ESS analysis of the abruptness parameter γ was undertaken by one of us (Getz, 1996), focusing mainly on the stability properties of the invasion or exclusion equilibrium $(\bar{x}, \bar{y})' = (K_1(r_1 - 1)^{1/\gamma_1}, 0)'$ of the competitive system

$$x_{t+1} = \frac{r_1 x_t}{1 + ((x_t + a_1 y_t)/K_1)^{\gamma_1}} \tag{2}$$

$$y_{t+1} = \frac{r_2 y_t}{1 + ((y_t + a_2 x_t)/K_2)^{\gamma_2}}, \tag{3}$$

in which x is regarded as the density of a resident population and y is regarded as the density of an invading mutant population. This analysis provided some new insights into the relationship between the abruptness of the onset of density dependence, as characterized by the parameter γ, and the per capita growth rate r. Specifically, it was demonstrated for $r > 2$ (i.e., the population has the potential to more than double each generation) that, if γ were allowed to assume its lower bound of 1, then the ESS is $\gamma = 1$. (Note that when $\gamma = 1$, the density-dependence in Eq. (1), is no longer inverse sigmoidal in that derivative of the growth rate is a maximum at the boundary $x = 0$.) For $1 < r < 2$, ESS solutions appear to exist, but they are difficult to find because of the chaotic dynamics of equation (1). It was also shown through direct numerical simulation that when $r = 1.5$ the ESS has the value $\gamma = 9.58$ correct to two decimal places. For this value of γ the onset of density dependence is relatively abrupt.

In this paper, we shift the emphasis of using the competitive system (2) and (3) to explore ESS solutions to Eq. (1) to other techniques of analysis, such as the use of invasion exponents (see Rand *et al.*, 1994)) and of strategy dynamics, as developed by Vincent *et al.* (1993). Although these approaches only yield candidate or "local" ESS solutions (referred to by Rand *et al.* as ESA or evolutionary stable attractors), we applied the methods over a broad range of initial conditions. Thus we are confident that, in most cases, we have found the actual ESS solutions. Throughout the paper, we refer to our solutions as ESS solutions, although we do not have analytical verification that our solutions satisfy the global exclusion property required for them to be ESSs.

We also apply the strategy dynamics approach to situations where the abruptness parameter γ is permitted to be an evolving function of time, or even to be a state-dependent function (i.e., $\gamma = (\gamma(x))$ with a form that may evolve with time. Further, we analyze the situation where a population is able to increase the value of γ only at the expense of its intrinsic growth rate r (i.e., $r = r(\gamma)$ and $dr/d\gamma < 0$ over some range of r). The reason for allowing γ to be a function of the population state x, rather than a constant, is that individuals may develop state-dependent strategies that are able to invade populations playing any constant strategy, including the ESS solution among the class of constant strategies.

One interpretation for γ close to 1 is that females clump their young on resources so that competition sets in among maturing individuals at relatively low densities, while for large γ the contrasting interpretation is that females over disperse their young (Getz, 1996) thereby delaying the onset of competition. Thus, it is quite possible that females could evolve a density-dependent rule relating to under or over dispersing their young on resources in response to adult population densities. From a mathematical point of view, our interest in time and state-dependent strategies is that they may have the effect of stabilizing the system or, at least, reducing the amplitudes of oscillations.

We begin our analysis, in Section 2, with application of the concepts of both invasion exponents and strategy dynamics to explore the possibilities of equilibrium, periodic and chaotic ESSs. Among other things, we show that interior ESSs (i.e., values on the open interval $(1, \infty)$) exist for $1 < r < 2$, but that they never produce stable population equilibrium dynamics: i.e., the ESS value γ^* never satisfies the equilibrium stability condition $\gamma < 2r/(r - 1)$ (Getz, 1996). On the other hand, when $r > 2$, the boundary value $\gamma = 1$ always is the ESS. Further, since $2r/(r - 1) > 1$ for all $r > 1$, this ESS satisfies the equilibrium stability condition and the system evolves to a stable population equilibrium solution.

Many organisms, including organisms such as cladocerans (Guisande, 1993), have reproductive strategies that depend on the density of their populations. Well-known examples among the insects include dung beetles

(Yasuda, 1990) and moths (Gage, 1995). Thus it makes senses from a biological point of view to consider strategy parameters to actually be functions of population density x. Here we considered the simple case where the abruptness parameter γ is a linear function of x. Thus, in Section 3, we consider the conditions under which a population playing an ESS from the class of constant γ can be invaded by a population playing a state-dependent function, in particular a linear function, $\gamma(x)$.

A third way that we view our system is by considering that an evolutionary trade-off exists between increasing the value of γ and increasing the value of r in model (1). For example, in the case where small γ corresponds to females clumping their young on resources, an investment in energy or even in improved sensory and perceptual systems is required for females to make the effort to over disperse their young on resources. Both cases require resources that could be used to increase the value of r. Further, females that tend to overdisperse their young are probably subject to higher levels of predation compared with females that tend to underdisperse their young. In this case, the expected value of r is reduced by increased mortality (the reproductive value of individuals in populations depends both on fecundity and mortality rates—see Getz and Haight (1989) or Caswell (1989)). Thus, in Section 4, we consider the situation where the value of r is inversely related to the value of γ and decreases from a maximum value r_0 at $\gamma = 1$ to a minimum value r_∞ as $\gamma \to \infty$.

Finally, in Section 5, we link the analysis in Sections 3 and 4 by considering the situation where r and γ are mutually interdependent in both being functions of the same parameter v that is itself a linear function of the state x. This provides an analysis of systems where growth and density dependence are mutually constrained, but a density-dependent evolutionary strategy is still possible.

2. AN ESS ANALYSIS OF THE BASIC MODEL

In this section, without loss of generality, we choose our unit of density to be units of K (equivalently, we set $K = 1$) in (1). Further, in keeping with the assumption that the resident and mutant phenotypes are identical except with respect to the parameter subject to evolutionary change, we consider the case $r_1 = r_2 = r$ and $a_1 = a_2 = K_1 = K_2 = 1$ in Eqs. (2) and (3). Thus, we consider an ESS analysis purely in terms of the density-dependent abruptness parameter γ.

2.1. Equilibrium ESSs

First, we explore the possibility that evolutionary stable γ strategies correspond to equilibrium solutions of the population equation (1). More precisely, we consider equilibrium solutions of the form $(x_t, y_r) = (\bar{x}, 0)$ of the competitive system (2) and (3), obtained by putting $x_{t+1} = x_t = \bar{x}$ and $y_{t+1} = y_t = 0$ in these two equations. If we henceforth denote the abruptness parameter of the resident phenotype by γ_R, and that of the mutant simply by γ, then we find that, for given values of r and γ_R,

$$\bar{x} = (r-1)^{1/\gamma_R}. \tag{4}$$

Note that $\bar{x}$ is also the equilibrium state of (1). The parameter γ_R is an ESS with corresponding resident equilibrium state $\bar{x}$, only if the following two conditions are satisfied (see Vincent *et al.* 1993; Vincent and Fisher, 1988):

1. The equilibrium solution $\bar{x}$ is an attractor of (1).
2. The fitness function

$$R(r, \gamma, \bar{x}) = \frac{r}{1 + (\bar{x})^{\gamma}} \tag{5}$$

is a maximum with respect to the parameter γ when $\gamma = \gamma_R$. It should be understood that the fitness function referred to here is actually that of the mutant phenotype, i.e., the one occurring in (3) with $y_t = 0$ and $x_t = \bar{x}$. (See also Ferrière and Gatto, 1995; Rand *et al.*, 1994.)

The usual practice in the literature, especially in the case of periodic or chaotic population states, is to carry out analysis in the context of the *invasion exponent*

$$I(r, \gamma, \bar{x}) = \log |R(r, \gamma, \bar{x})| \tag{6}$$

rather than the fitness function R (see Rand *et al.*, 1994; Ferrière and Gatto, 1995, for more details). For the sake of uniformity we will follow the same practice. Since the invasion exponent procedure only identifies potential ESS solutions (the conditions relate to invasions by local or nearby strategies), we used numerical simulations of Eqs. (2) and (3) to verify that the ESS solutions did apply globally.

For the equilibrium point $\bar{x}$ to be an attractor of (1), it must satisfy the condition

$$\left| \frac{\partial}{\partial x} \left[\frac{rx}{1 + x^{\gamma_R}} \right]_{x=\bar{x}} \right| < 1. \tag{7}$$

Using (4), this inequality becomes

$$\left|1-\frac{\gamma_R(r-1)}{r}\right|<1, \tag{8}$$

or

$$0<\frac{\gamma_R(r-1)}{r}<2. \tag{9}$$

This implies that $\bar{x}$ would only be an attractor if

$$r>1 \quad \text{and} \quad \gamma_R<\frac{2r}{r-1}. \tag{10}$$

Next define the function

$$s(\gamma)=\frac{\partial}{\partial\gamma} I(r, \gamma, \bar{x}) \tag{11}$$

referred to by Rand *et al.* (1994) as the differential selective pressure.

The second condition for an ESS can be satisfied in one of two ways:

1. If $s(\gamma_R)=0$ and $s'(\gamma_R)<0$ for some γ_R in the interval $(1, \infty)$. In this case we refer to the ESS as an interior ESS.

2. If we include $\gamma=1$ as a possible value, and $s(1)<0$, then $I(r, \gamma, \bar{x})$ will be a decreasing function of γ, and hence take on a maximum value at the left boundary $\gamma \to 1$. In this case we say that a boundary ESS occurs.

In the case of the model (1), with $\bar{x}$ given by (4),

$$s(\gamma)=\frac{(-1/\gamma_R)(r-1)^{\gamma/\gamma_R}\log(r-1)}{1+(r-1)^{\gamma/\gamma_R}}. \tag{12}$$

Thus, on putting $\gamma=\gamma_R$, we obtain

$$s(\gamma_R)=-\frac{1}{r\gamma_R}(r-1)\log(r-1) \tag{13}$$

and

$$s'(\gamma_R)=-\frac{(r-1)[\log(r-1)]^2}{\gamma_R^2 r^2}. \tag{14}$$

Since $s'(\gamma_R) \propto s(\gamma_R)^2$, the conditions $s(\gamma_R)=0$, $s'(\gamma_R)<0$ can never both be satisfied. Thus there is no equilibrium interior ESS on the interval $1<\gamma<\infty$. If $1<r<2$, then $s(\gamma)>0$ for all γ. Thus $I(r, \gamma, \bar{x})$ is monotonically increasing for values of γ up to the period-doubling bifurcation and beyond. Thus for these values of r neither an interior nor a boundary ESS exists for $1<\gamma<\infty$. When $r=2$, $s(\gamma)=s'(\gamma)$ for all γ. In this case $\bar{x}=K=1$, and the parameter γ is evolutionary neutral. When $r>2$ we see that $s(\gamma)<0$ for all $\gamma>1$ and therefore, in particular, $s(1)<0$. Thus a boundary ESS occurs at the left boundary $\gamma \to 1$ when $r>2$. This agrees with the results obtained previously by Getz (1996) through simulation of the competitive Eqs. (2) and (3). Note that if the constraint were $\gamma \geqslant 0$ (see Eq. (1)) then the boundary ESSs would occur at $\gamma \to 0$ instead of $\gamma \to 1$. As discussed in the Introduction, however, the parameter range $0 \leqslant \gamma < 1$ is not biologically plausible.

2.2. Period Two ESSs

In the absence of an ESS that corresponds to an equilibrium of the model (1), the least complex of the remaining possibilities is an ESS $\gamma_R=\gamma^*$ that corresponds to a period two attractor; i.e., an attractor consisting of the two points $\{x_0, x_1\}$ such that

$$x_1=rx_0/(1+x_0^{\gamma^*}), \qquad x_0=rx_1/(1+x_1^{\gamma^*}), \tag{15}$$

and the stability conditions

$$\left|\frac{\partial}{\partial x}\left[\frac{rx}{1+x^{\gamma^*}}\right]_{x=x_0}\frac{\partial}{\partial x}\left[\frac{rx}{1+x^{\gamma^*}}\right]_{x=x_1}\right|<1 \tag{16}$$

are satisfied. In this case the invasion exponent is

$$I(r, \gamma, x_0, x_1)=(1/2)\left[\log\left|\frac{r}{1+x_0^{\gamma}}\right|+\log\left|\frac{r}{1+x_1^{\gamma}}\right|\right], \tag{17}$$

and the selective differential pressure is

$$\begin{aligned} s(\gamma)&=\frac{\partial}{\partial\gamma} I(r, \gamma, x_0, x_1) \\ &=-\frac{1}{2}\left[\frac{x_0^{\gamma}\log x_0}{1+x_0^{\gamma}}+\frac{x_1^{\gamma}\log x_1}{1+x_1^{\gamma}}\right]. \end{aligned} \tag{18}$$

As before, the invasion exponent must take a maximum value (of 0) with respect to γ at $\gamma=\gamma_R=\gamma^*$, which adds the conditions

$$s(\gamma^*)=0 \tag{19}$$

and

$$s'(\gamma^*) < 0 \tag{20}$$

to (15) and (16).

To solve for a period two ESS, we proceeded as follows. We used the Maple (Ellis *et al.*, 1992) nonlinear equation solver to solve Eqs. (15) and (19) simultaneously for x_0, x_1 ($\neq x_0$) and γ^* for a given value of r. We then tested this to see whether it satisfied the constraints (16) and (20). If it did, then we could conclude that γ^* is at least a local ESS, and the corresponding period two state is $\{x_0, x_1\}$.

In Appendix A, we demonstrate that real solutions of (15) and (19), satisfying the constraints, can only be found if $1.6494 < r < 2$. Thus, the corresponding ESS values of γ (Table 1) are the only values of γ for which a period two ESS exists. The sequence A in Fig. 1 is a plot of these period two ESS values of γ corresponding to particular values of r. The vertical dashed line at $r = 1/6494$ marks the left boundary of this period two sequence. Note, this boundary is also the point where the period two ESS states bifurcate to period four ESS states.

It is also worth noting that in the limit as $r \to 2$, the period two solutions and corresponding ESS satisfy x_0, $x_1 \to 1$ and $\gamma^* \to 4$. This is a particularly interesting result, since Eqs. (15) are satisfied for all values of γ^* when $r = 2$ and $x_0 = x_1 = 1$, but numerical simulations reveal that only $\gamma^* = 4$, is the ESS. Thus, as $r \to 2$ from above, the equilibrium boundary ESS $\gamma^* = 1$ is lost at $r = 2$: it jumps to the value $\gamma^* = 4$ and, in the processes, the corresponding state bifurcates from an equilibrium to a period two solution. In this sense $r = 2$ is a singularity of the system.

TABLE 1

Constant ESS Strategies γ* Yield Period Two Dynamics for a Range of Growth Rate Values *r* in Model (1) (with $K = 1$)

r	γ^*	x_0	x_1
1.64941	6.5030	0.713007	1.058698
1.6495	6.5017	0.713029	1.058726
1.6	7.1687	0.703837	1.044793
1.65	6.4950	0.713140	1.058864
1.7	5.9041	0.726165	1.042345
1.75	5.4343	0.743183	1.084447
1.8	5.0497	0.764818	1.094133
1.85	4.7272	0.792275	1.099857
1.9	4.4515	0.827987	1.098894
1.95	4.2118	0.878057	1.084864

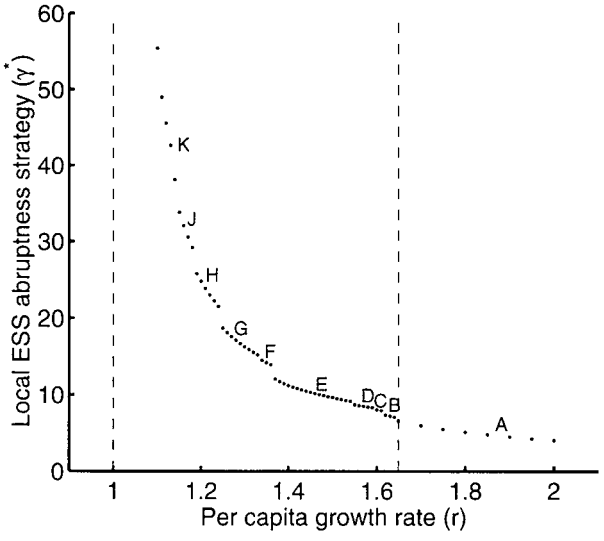

FIG. 1. ESS strategies γ^* for the model (1) for various values of r in the range $1 < r \leqslant 2$. The sequence A is the set of period two ESSs shown in Table 1, together with the ESS $\gamma^* = 4$ at $r = 2$. The sequences B through K denote ESSs with more complex density states, as explained in the text. The vertical dashed line between sequences A and B shows the period four bifurcation point $r = 1.64941$.

2.3. Higher Periods and Chaos

Since neither an equilibrium nor a period two ESS is possible for $r \leqslant 1.6494$, any ESS for these values of r, if it exists at all, would have to correspond to a more complex state. Using a more general definition of the invasion exponent I and selective differential pressure s than defined by Eqs. (17) and (18), respectively (see Rand *et al.*, 1994; Ferrière and Gatto, 1995) it would be possible to extend the analysis above to higher period attractors and even chaotic attractors.

We preferred to use instead an alternative method to obtaining ESS values for γ that is computationally efficient for problems where the ESS value corresponds to complex or chaotic solutions, and which is based on an approach developed by Vincent and others (Vincent, 1990; Vincent *et al.*, 1993; Getz and Kaitala, 1993). This approach is in fact not so much a computational technique as an actual model of evolution of a strategy with time. It can be concisely formulated as follows: If the population model is given by

$$x_{t+1} = R(x_t, u)\, x_t, \tag{21}$$

where u is a parameter (strategy), which can change through the course of evolution, then the approach of Vincent *et al.* (1993) considers u to be time dependent,

and models the evolution of both x and u by means of the system

$$\begin{aligned} x_{t+1} &= R(x_t, u_t)\, x_t \\ u_{t+1} &= u_t + \frac{\sigma^2}{R}\left[\frac{\partial R}{\partial u}\right]_{u=u_t,\, x=x_t}. \end{aligned} \tag{22}$$

Here u_t is actually equal to the mean of the various values of the strategy u played by the individual members of the species considered, and σ^2 is the variance. This model was derived under the assumptions that u is distributed symmetrically about the mean, and that the variance σ^2 is small. Under these assumptions σ^2 can be shown to remain constant. In actual populations this would not generally be true. One might expect during the course of evolution that most members of the species eventually adopt the most successful strategy so that the variance is, in fact, a decreasing function of time. This conclusion is in fact a direct consequence of Fisher's Fundamental Theorem of Natural Selection which, to quote Sober (1984, p. 178), is that "the rate of increase of fitness in a population at any point in time equals the additive genetic variance at that time." However, if σ^2 is sufficiently small to begin with, it would not matter significantly whether it is constant or not from a modeling point of view.

Again, one has to be careful that the candidate ESS solutions derived from Eqs. (22) do in fact apply globally before concluding that they indeed are ESS solutions. We did this by checking that the equations converged to the same solution from several different sets of contrasting initial conditions.

It is not difficult to see (Vincent *et al.* 1993) that a stable fixed point of this system will correspond to an equilibrium interior ESS of the model (21) with respect to the strategy u. Moreover, if there is a boundary ESS on either the left or right boundary, u_t would evolve to that boundary if u_0 is sufficiently close to it.

It can also be shown, however, that a stable n-periodic solution of (22) will correspond to a n-periodic interior ESS of the model (21) with respect to strategy u, in the limiting case $\sigma^2 \to 0$, and that solutions to Eqs. (22) will evolve to a boundary ESS if it exists, and if u_0 is near enough to that boundary. A proof of this is given in Appendix B. If Eq. (21) has an ESS with respect to u corresponding to a chaotic attractor, solutions to Eqs. (22) will at least converge to a value of u very near to this ESS value. A heuristic argument to explain this is also given in Appendix B. Thus Eqs. (22) can also be used to simulate evolution towards a periodic or chaotic ESS. It can also be viewed as a computational tool to calculate ESS values of u.

In cases where solutions to Eqs. (22) converge to more than one solution, these candidate ESSs (or ESAs in the sense of Rand *et al.*, 1994) can be played against one another to check which of them is the actual ESS. In some situations, as discussed below, both potential ESSs resist invasion by the other, in which case they are actually coexisting ESSs (Vincent *et al.* 1996) with the one that establishes itself first for a particular evolutionary system being the one to prevail in the end.

Let us return now to the model (1), for which $u = \gamma$, and $R(x, \gamma) = r/(1 + x^\gamma)$. In this case, the evolutionary system (22) takes the form

$$\begin{aligned} x_{t+1} &= \frac{r x_t}{1 + x_t^{\gamma_t}} \\ \gamma_{t+1} &= \gamma_t - \frac{\sigma^2 x_t^{\gamma_t} \log x_t}{1 + x_t^{\gamma_t}}. \end{aligned} \tag{23}$$

To obtain an accurate value of γ which corresponds to a periodic or chaotic ESS of (1), it is necessary to use as small a value of σ^2 as possible. Unfortunately, a small value of this parameter also means very slow convergence. However, if the system (23) is viewed as a computational method, rather than an evolutionary model, the parameter σ^2 could be made a decreasing function of time.

One approach is to start with a value of $\sigma^2 = 1$, say, and to calculate the values of x_t and γ_t from (23) until γ_t stabilizes into some periodic or chaotic state. We then decrease σ^2 to a value of 0.1, say, and continue the process. This is repeated, with ever decreasing σ^2, until γ is as close to a constant value as desired. Another approach is to put

$$\sigma^2 = a e^{-bt}, \tag{24}$$

with a relatively large, and b relatively small and positive. This works fairly well, although perhaps not so accurately as the step wise decreasing approach described above. For example, when we set $a = 10$, $b = 0.01$ and $r = 1.8$, with $x_0 = 0.8$ and $\gamma_0 = 8$, we were able to calculate the ESSs in Table 1 correctly to two decimal places (i.e., a relative error of 0.155%) within 1245 generations (i.e., $t = 1245$). With a small constant σ^2, or even with a step wise decreasing one, an additional decimal place could be obtained, but only after a much longer time (of the order of $t = 30{,}000$ or more). A good compromise is to decrease σ exponentially, as above, but to switch to a constant value once σ reaches a given small value.

Using the above strategy dynamics approach, we were able to calculate a value of $\gamma = 9.58$ for the chaotic ESS at $r = 1.5$. This agrees with the value reported previously by Getz (1996). For $r = 1.2$, the ESS solution has very nearly a period five structure with intermittent chaos, and $\gamma = 24.75$ (Fig. 2).

These, and numerous other ESSs are shown in Fig. 1. The initial value for each ESS computation was either $\gamma_0 = 4$ in the case of larger values of r, or the result of the previous computation in the case of smaller values of r. Note that this $r - \gamma^*$ bifurcation diagram consists of several smooth sections, labeled B through K, with rapid "jumps" in γ^* between these sections. Sequence B starts with a period four ESS at $r = 1.6494$, followed rapidly by period 8 and eventually a chaotic ESS as r decreases. Note that sequence B does not line up smoothly with the period two sequence A. The short sequence C starts with a period five, followed by a quasi-periodic ESS as r decreases. The sequence D starts with chaotic states, but as r decreases, the states become almost period seven with intermittent chaos, and eventually exactly period seven. Sequence *E* also starts with chaotic states, and as r decreases, the states first become period three with intermittent chaos, and eventually exactly period three. Sequence *F* consists of states which are period seven with intermittent chaos, with the chaotic parts becoming less as r decreases. Sequence G. H and J consists respectively of almost period 4, 5 and 6 states with intermittent chaos, and once more the chaotic parts become less frequent as r decreases. In the case of G a pure period four state was eventually observed. In sequence K the states are almost all periodic with intermittent chaos, but the periods of the states increase rapidly but linearly as r decreases, i.e., period 7 is followed by period 8, 9, 10, etc.

In summary, the ESS γ^* always increases with decreasing r, and tends to infinity as r tends to the value $r = 1$. Except for the two sequences B and C near the period two bifurcation point, each sequence is more chaotic for higher values of r, and less chaotic but more periodic for lower values of r. For values of r between 1 and about 1.33, the periodicity of the ESS states increase as r decreases. Very near to $r = 1$ (not shown in the figure) there is generally no chaos at all, but periodic states with high periodicity.

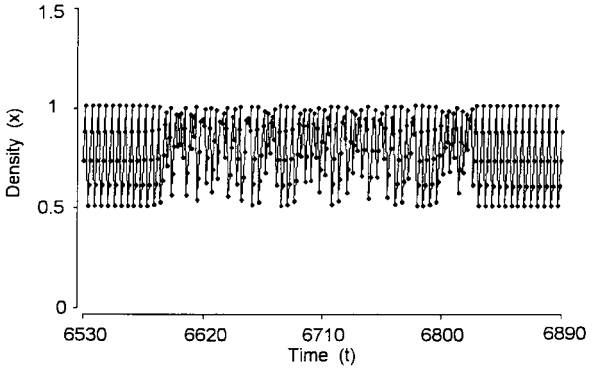

FIG. 2. Part of the time series generated by the model (1) when $r = 1.2$, and γ has its ESS value $\gamma = 24.75$.

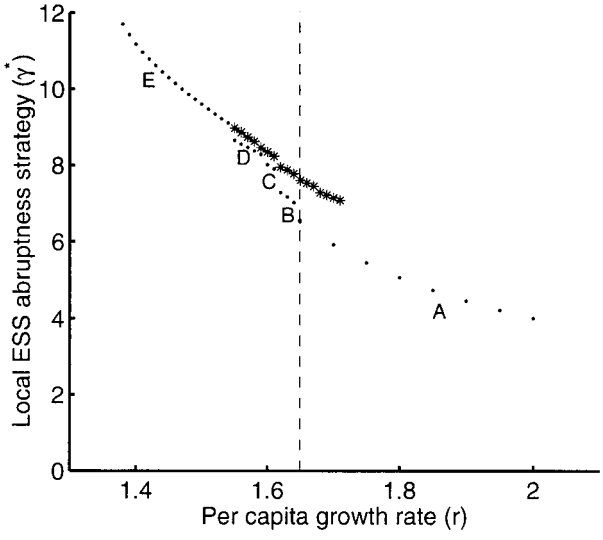

FIG. 3. Coexisting ESSs for the model (1) for some values of r. A, B. C, D, and E have the same meaning as in Fig. 1.

We also tried to find coexisting local ESSs. For initial values of γ between 4 and the ESS values shown in Fig. 1, the strategy dynamics iteration always converged to these ESS values. However, when using larger initial values of γ, some coexisting ESSs were found. These are shown in Fig. 3 as stars. These ESS states are invariably chaotic, and extend into the period two region of Fig. 1, where they vanish abruptly at about $r = 1.71$. At the left end they join the sequence E smoothly, and seem to form an extension of the chaotic ESS states at the right end of E. As mentioned above, these coexisting ESSs resist invasion by one another.

3. DENSITY DEPENDENT γ

A question that has received almost no attention is the extension of ESS analysis to strategies that depend on the density of the populations involved (but see Kaitala *et al.*, 1997). Here we explore the conditions under which a resident species modeled by (1), playing an ESS in the class of constant γ, can be invaded by a mutant playing a density-dependent γ which is specifically a linear function of density.

To investigate this, we express the parameter γ as the linear function

$$\gamma_t = mx_t + c, \tag{25}$$

where now the ESS values of m for given c, and c for given m are of interest. Of course, we are ultimately interested in the ESS values of m and c considered together.

In this case, Eq. (1) has the form

$$x_{t+1} = \frac{rx_t}{1 + x_t^{mx_t + c}}, \quad mx_t + c > 1. \tag{26}$$

The values of the parameters m and c that induce stable equilibrium, period two, and period four solutions for the case $r = 1.8$ are illustrated in Fig. 4. The three boundaries shown were generated by first calculating to four decimal places a number of points on each boundary, and then fitting a straight line through each set of points by least squares regression, which produced the equations

$$m = 4.966 - 1.106c,$$

Equilibrium/period two boundary (27)

$$m = 6.154 - 1.106c,$$

Period two/period four boundary (28)

$$m = 6.472 - 1.053c,$$

Period four/period eight boundary. (29)

The r^2 values indicate that the deviation from linearity is very slight. This is also clear from Fig. 4. These lines are almost, but not quite parallel. The line of equilibrium states for which $\gamma = m\bar{x} + c = 1$ is also shown in Fig. 4. This is in fact the line

$$m(r-1) + c = 0.8m + c = 1, \tag{30}$$

since the equilibrium state is easily seen to be $\bar{x} = r - 1$ when $m\bar{x} + c = 1$.

In our first set of ESS calculations for this model, we kept c mixed at various values, and allowed m to find an ESS value, using the equations

$$x_{t+1} = \frac{rx_t}{1 + x_t^{m_t x_t + c}} \tag{31}$$

$$m_{t+1} = m_t + \sigma^2 \frac{\partial}{\partial m} \left[\sum_{j=0}^{3} \log |\tilde{R}(x_{t-j}, m_t, c)| \right] \Big/ 4, \tag{32}$$

(33)

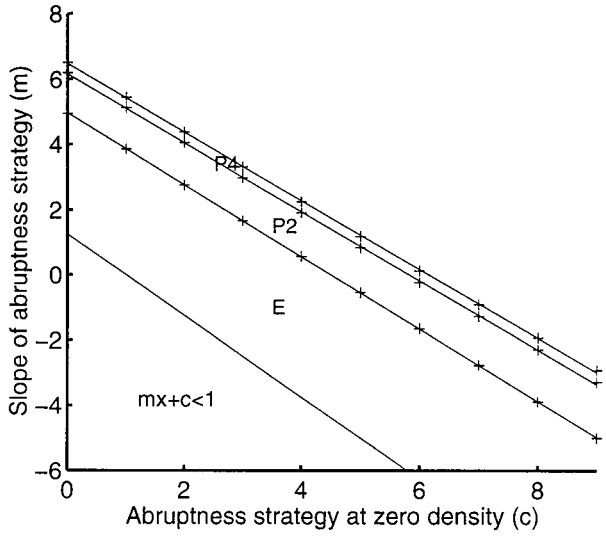

FIG. 4. Stability regions for equilibrium (E), period two (P2) and period four (P4) solutions of model (26) when $r = 1.8$.

where

$$\tilde{R}(x, m, c) = \frac{r}{1 + x^{mx + c}}. \tag{34}$$

Equation (31), which is an extension of Eq. (22), explicitly contains an invasion exponent appropriate for periodic solutions up to period four. This allows faster convergence towards an ESS than using (22).

We calculated values of m obtained in this way for given values of c and $r = 1.8$, as well as the minimum and maximum values x_{min} and x_{max} of x of the corresponding periodic attractor and the amplitude of oscillation, defined here as $(x_{max} - x_{min})/2$ (Table 2). In all cases, except when $c = 0$, 27 and 27.5, x_t converged to a period two solution. For $c = 0$ and 27 the attractor is period four, and for $c = 27.5$ we have what seems to be a periodic attractor of very high period. Beyond 27.5, γ_{min} rapidly approaches the lower bound $\gamma = 1$ of the model. Even though c was kept fixed, the derivative with respect to c of the invasion exponent

$$\left[\sum_{j=0}^{3} \log |\tilde{R}(x_{t-j}, m_t, c)| \right] \Big/ 4 \tag{35}$$

was monitored and was observed to decrease steadily with c from a value of 0.0087 at $c = 0$, to 0.003 at $c = 27$. Thus the invasion exponent forms a very flat surface above the m-c plane, with little variation in its gradient.

We also performed a set of calculations in which m was fixed at specific values and c was allowed to converge to

TABLE 2

ESS Values m^* When $r = 1.8$ and c Is Kept Fixed, as Well as the Bounds of the Corresponding Attractor of γ, and the Amplitude $(x_{max} - x_{min})/2$ of the Oscillation

Fixed c	ESS m^*	x_{min}	x_{max}	γ_{min}	γ_{max}	Amplitude
0	6.330	0.803	1.089	5.081	6.891	0.143
1	4.853	0.760	1.072	4.689	6.202	0.156
2	3.526	0.772	1.073	4.718	5.781	0.151
3	2.243	0.782	1.074	4.755	5.408	0.146
4	1.006	0.793	1.074	4.797	5.081	0.141
5	−0.194	0.802	1.075	4.792	4.844	0.136
5.04967[a]	−0.253	0.803	1.075	4.778	4.847	0.136
6	−1.363	0.811	1.075	4.535	4.895	0.132
7	−2.507	0.819	1.074	4.307	4.948	0.128
8	−3.629	0.826	1.074	4.307	4.948	0.124
9	−4.735	0.833	1.073	3.918	5.056	0.120
10	−5.826	0.839	1.073	3.749	5.112	0.117
15	−11.141	0.863	1.069	3.086	5.384	0.103
20	−16.322	0.880	1.066	2.602	5.639	0.093
25	−21.438	0.892	1.063	2.218	5.876	0.085
27	−23.339	0.886	1.088	1.615	6.314	0.101
27.5	−23.438	0.878	1.123	1.179	6.913	0.122

[a] The case $c = 5.04967$, $m = 0$ corresponds to the constant ESS case $\gamma^* = 5.04967$. In the linear case, however, m^* evolves to -0.253 rather than 0.

an ESS value c^*. In this case we used the equations (recall expression (34))

$$x_{t+1} = \frac{rx_t}{1 + x_t^{mx_t + c_t}} \tag{36}$$

$$c_{t+1} = c_t + \sigma^2 \frac{\partial}{\partial c}\left[\sum_{j=0}^{3} \log |\tilde{R}(x_{t-j}, m, c_t)|\right] \Big/ 4. \tag{37}$$

Once again x_t converged to a period two solution in all cases (Table 3), except for $m = -23$, where it converged to a period 12 solution, and $m = 4$, 5 and 6, where it converged to a chaotic solution. The derivative of the invasion exponent with respect to m was monitored this time and varied from a value of -0.004 at $m = -16$ to -0.010 at $m = 3$. (We did not attempt to calculate this derivative for states more complex than period four.)

Figure 5 shows the ESS m values of Table 2 plotted against fixed values of c, and the fixed values of m in Table 3 plotted against the corresponding ESS c values. Note that the two sets of points form two distinct curves, which never intersect each other.

An examination of the numbers in both Tables 2 and 3 show the following:

TABLE 3

ESS Values c^* When $r = 1.8$ and m Is Kept Fixed, as Well as the Bounds of the Corresponding Attractor of γ, and of the Amplitude $(x_{max} - x_{min})/2$ of the Oscillation

Fixed c	ESS c^*	x_{min}	x_{max}	γ_{min}	γ_{max}	Amplitude
−23	26.918	0.886	1.097	1.689	6.534	0.105
−16	19.855	0.876	1.079	2.588	5.842	0.102
−14	17.899	0.869	1.082	2.757	5.738	0.106
−10	14.029	0.850	1.087	3.159	5.523	0.118
−5	9.333	0.816	1.093	3.868	5.251	0.138
−2	6.688	0.787	1.095	4.498	5.113	0.154
−1	5.854	0.776	1.095	4.759	5.078	0.159
0.01	5.042	0.765	1.094	5.049	5.053	0.165
0.1	4.971	0.764	1.094	5.047	5.080	0.165
0.2	4.893	0.762	1.094	5.045	5.111	0.166
0.3	4.815	0.761	1.094	5.043	5.143	0.166
0.4	4.737	0.760	1.094	5.041	5.174	0.167
1	4.277	0.753	1.093	5.030	5.370	0.170
2	3.537	0.741	1.091	5.019	5.720	0.175
3	2.828	0.730	1.089	5.018	6.097	0.180
4	2.79	0.563	1.141	5.045	7.357	0.289
5	2.00	0.544	1.142	4.725	7.713	0.299
6	1.18	0.532	1.140	4.371	8.018	0.304

1. The values of x_{min} and x_{max} are relatively insensitive to variations in c and m.

2. The amplitude of the attractor (as defined above) decreases steadily when m decreases, except in some cases when the attractor becomes more complex ($c = 0$, 27 and 27.5 in Table 2 and $m = -23$, but not $m = 4$, 5 and 6 in Table 3).

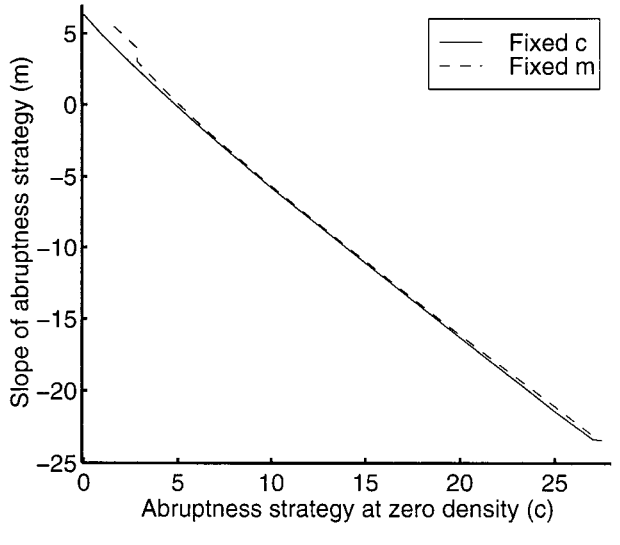

FIG. 5. ESS values m^* shown in Table 2 are plotted as a solid curve for a sequence of fixed values of c in the model (26), while the ESS values c^* showed in Table 3 are plotted as a dashed curve for a sequence of fixed values of m.

3. The minimum value of γ, γ_{min}, decreases steadily as m decreases.

To see how a population governed by the model (26) would compete with one governed by model (1), we considered the system

$$x_{t+1} = \frac{rx_t}{1+(x_t+y_t)^{\gamma}}$$
$$y_{t+1} = \frac{ry_t}{1+(x_t+y_t)^{m(x_t+y_t)+c}}. \tag{38}$$

For $r = 1.8$ we put $\gamma = 5.04967$, the ESS value from Table 1, and m and c were first given values from Table 2. In all (and *only*) the cases where m is negative, the population with density y_t invaded the population with density x_t for any $y_0 > 0$. (We put $x_0 = 0.89$ throughout.) In the case where $c = 5$, both the resident and the invader settled into patterns that persisted for at least 100,000 generations, but for higher values of c (and more negative values of m) the resident population x_t was totally replaced by the invader y_t. The rate at which invasion took place became larger with increasing c: at $c = 6$ it took 4490 time steps (generations) for x_t to become less than 10^{-12}, but at $c = 27.5$ it took only 370 time steps. When running the competition model (38) with the values of m and c in Table 3, similar results were obtained: again only the negative values of m led to invasion and replacement of the resident population, and the rate of invasion became larger as m decreased (and c increased).

Finally we played the strategies in both tables against each other by means of the competition model

$$x_{t+1} = \frac{rx_t}{1+(x_t+y_t)^{m_1(x_t+y_t)+c_1}}$$
$$y_{t+1} = \frac{ry_t}{1+(x_t+y_t)^{m_2(x_t+y_t)+c_2}}. \tag{39}$$

These simulations showed that a population with a lower value of m always invaded a population with a higher value of m. Thus the most successful strategies in both tables are those with the largest values of c and the lowest (negative) values of m. The more successful strategies also tend to have smaller amplitudes of oscillation for x_t.

As a next step in calculating ESS values for the model (26), we allowed both m and c to evolve towards possible ESS values, using the strategy dynamics system

$$x_{t+1} = \frac{rx_t}{1+x^{mx_t+c_t}}$$
$$m_{t+1} = m_t + \sigma^2 \frac{\partial}{\partial m}\left[\sum_{j=0}^{3} \log|\tilde{R}(x_{t-j}, m_t, c_t)|\right] \Big/ 4 \tag{40}$$
$$c_{t+1} = c_t + \sigma^2 \frac{\partial}{\partial c}\left[\sum_{j=0}^{3} \log|\tilde{R}(x_{t-j}, m_t, c_t)|\right] \Big/ 4.$$

This system was designed to maximize the appropriate invasion exponent with respect to both m and c for periodic solutions up to period four.

Despite the use of many different starting configurations, the system would never converge. Instead c_t increased and m_t decreased steadily, until the constraint $\gamma > 1$ terminated the iterations (i.e, the iterations was stopped just before the minimum value of $\gamma = mx + c$ became equal to or less than one). This, in conjunction with the results reported above when fixing either c or m, implies that model (26) has no interior ESS, only a boundary ESS constrained by the condition $\gamma > 1$.

It is difficult to find this boundary ESS exactly, since the boundary on the m-c plane itself is difficult to find. We attempted to get at least an indication of the ESS values, by using the results in Tables 2 and 3 as a guide. When using the values $m = -23.339$, $c = 27$ and $x = 0.886$ from Table 2 as the starting values m_0, c_0 and x_0, the constraint $\gamma > 1$ stopped the iterations when $c_t = 28.489$ and $m_t = -24.441$. At this time the minimum value of γ was 1.0001, and the maximum value was 6.992. When using $m = -23$, $c = 26.918$ and $x = 0.886$ from Table 3 as starting values, the iterations were stopped at $c_t = 28.752$ and $m_t = -24.758$, with γ varying between 1.0004 and 6.943 as x oscillates between its maximum and minimum values. Simulation of the system (40) indicated that, of the two sets of values of m and c, the last one with its more negative m is also the more successful.

For $r = 1.5$ (for which the constant γ model (1) has an ESS $\gamma = 9.58$, corresponding to a chaotic state) similar calculations were performed. Some of them are shown in Table 4. Again the most successful strategies were those with the most negative values of m, and γ_{min} near one.

When using Eqs. (40), we still could not find an interior ESS, although a boundary ESS seems to exist, as in the case $r = 1.8$. The most successful strategy we found was calculated by means of Eqs. (40), using $m = -27$, $c = 29.39$ and $x = 0.765$ s starting values. The values of m and c calculated in this way were $m = -27.360$ and $c = 9.545$, and for these values γ varies between 1.00001 and 8.590.

The results for $r = 1.5$ are very similar to those for $r = 1.8$. Again the best strategy is one with a minimum γ

TABLE 4

ESS Values c^* When $r = 1.5$ and m Is Kept Fixed (Top) and Vice Versa (Bottom), as Well as the Bounds of the Corresponding Attractor and of γ, the Amplitude of the Corresponding Oscillation, and the Type of Attractor

		x_{min}	x_{max}	γ_{min}	γ_{max}	Amplitude	Type
Fixed c	ESS m^*						
9.58	−0.034	0.545	1.073	9.444	9.719	0.264	Chaotic
20	−12.16	0.585	1.091	6.738	12.891	0.253	Chaotic
28	−25.81	0.760	1.036	1.257	8.393	0.138	Period 2
29	−26.99	0.764	1.037	1.003	8.389	0.137	Period 2
Fixed m	ESS c^*						
−27	29.39	0.765	1.047	1.130	8.743	0.141	Period 2
−25	27.67	0.757	1.044	1.569	8.757	0.144	Period 2
−20	23.63	0.737	1.037	2.896	8.891	0.150	Period 2
−5	14.00	0.543	1.084	8.582	11.291	0.271	Chaotic

which approaches one, and with a low negative value of m. The amplitude of the oscillations decreases steadily as m decreases towards its boundary ESS value as before.

The differences here, however, are the following:

1. For $r = 1.8$ the density x_t evolved from period 2 to a more complex state. For the case $r = 1.5$, it is the other way around: the state evolved from a chaotic to a less complex period two state.

2. For $r = 1.5$, the lower bound x_{min} of the attractor is more sensitive to changes in c and m than for the case $r = 1.8$.

For several other values of r in the range $1 < r < 2$ we also failed to find an interior ESS, but did confirm the existence of a boundary ESS with a negative value of m. For $r = 2$, system (40) does converge to an interior ESS. This ESS corresponds to the equilibrium state $x = 1$, and the ESS values of m and c depend on the initial values used for Eq. (40), but they always produce a constant value of $\gamma = 4.000$. This is essentially the same ESS as for the constant γ model (1) when $r = 2$. Finally, for $r > 2$ only equilibrium boundary ESSs exist, which therefore also correspond to the equilibrium boundary ESSs for (1).

The results of this section can be summarized as follows. For values of r larger than 2 the ESSs correspond to the same equilibrium states as for the constant γ model (1). In this case, the ESS is the boundary limit value $\gamma = 1$. For smaller values of r (i.e., $1 < r < 2$), a linear $\gamma = mx + c$ produces an ESS that outcompetes the constant ESS (as it must since the constant case is just a special linear case). The best linear density-dependent strategies correspond to periodic or chaotic states with relatively small amplitudes of oscillation about the maximum carrying capacity, and a value of γ which is as close as possible to the lower bound $\gamma = 1$ when the density is a maximum, and relatively large (i.e., around 5 to 10 for r around 1.5 to 1.8) when the density is a minimum.

4. GROWTH RATE IS A FUNCTION OF ABRUPTNESS

The basic model (1) studied so far does not admit interior ESS solutions that produce equilibrium dynamics, except when $r = 2$. Further, when $1 < r < 2$ this model does not even admit boundary ESS solutions with equilibrium dynamics. It is still a matter of controversy whether an actual biological system evolves towards chaotic dynamics, and some biologists favor models producing equilibrium ESS states. In this context Doebeli (1995), for example, introduced an ad hoc feedback controlling mechanism into the model (1) to force the system to be stable. It could be argued that such a model should at least admit the possibility of equilibrium ESSs so that it might be used to explore the various possibilities.

We asked the question whether model (1) would behave in a more stable fashion if the values of r and γ were linked. From a biological point of view, it is reasonable to assume that the value of r is related in some way to the value of the abruptness parameter γ. In fact, as discussed in the Introduction, we may expect that r and γ are inversely correlated: If a species invests in reducing the onset of density dependence, then it may well be doing so at the expense of its intrinsic growth. This link is easily made if we assume that

$$\gamma(v) = 1 + v, \tag{41}$$

where $v>0$ is a parameter related to "investment in delaying the onset of density dependence," and assume that $r=r(v)$ is a decreasing function of v. In this case we have a trade-off between the $r(v)$ and $\gamma(v)$ and model (1) takes the form

$$x_{t+1}=\frac{r(v)\,x_t}{1+x_t^{1+v}},\quad v>0. \tag{42}$$

One possible form for $r(v)$ is

$$r(v)=\frac{r_0}{1+(v/q)^p}. \tag{43}$$

For $p>1$, $r'(0)=0$, and $r(v)$ then has an inverted sigmoid form in the $r-v$ plane. Larger values of q increases the length of the initially almost constant part of $r(v)$ and, for larger values of p, the rapidly descending middle part of the curve becomes steeper.

We first investigate the possibility of an equilibrium ESS for this model. As before, we denote the strategy of the resident by v_R, and that of the mutant by v. An equilibrium solution of (42) corresponding to resident strategy v_R is

$$\bar{x}=[\,r(v_R)-1\,]^{1/(1+v_R)}. \tag{44}$$

The invasion exponent is given by (6), with

$$R(r_0,\,p,\,q,\,v,\,\bar{x})=\frac{r(v)}{1+\bar{x}^{1+v}}. \tag{45}$$

The selective differential pressure is then

$$\begin{aligned} s(v)&=\frac{d}{dv}\log|R|=\frac{\left[\dfrac{\partial R}{\partial v}\right]_{x=\bar{x}}}{R}\\ &=\frac{r'(v)}{r(v)}-\frac{\bar{x}^{1+v}\log\bar{x}}{1+\bar{x}^{1+v}}, \end{aligned} \tag{46}$$

where

$$r'(v)=-pr_0v^{p-1}q^p/(q^p+v^p)^2. \tag{47}$$

Then, using (44), the condition $s(v_R)=0$ for an ESS resident strategy $v_R=v^*$ becomes the transcendental equation

$$(1+v^*)\,r'(v^*)-(r(v^*)-1)\log(r(v^*)-1)=0. \tag{48}$$

At the same time the inequality $s'(v_R)=s'(v^*)<0$ must also be satisfied and, if the system is to be stable, the stability condition

$$\begin{aligned} D_1&=\left[\frac{d}{dx}\left(\frac{xr(v^*)}{1+x^{1+v^*}}\right)\right]_{x=\bar{x}}\\ &=1-\frac{[\,v^*+1\,][\,r(v^*)-1\,]}{r}<1 \end{aligned} \tag{49}$$

must hold.

Unlike the case for constant r, an ESS that produces an equilibrium system now exists for a range of values of the various parameters in $r(v)$, as can be seen in Figs. 6 and 7. We can similarly identify ESS solutions that produce period two system dynamics. This identification is made by first solving the equations (cf. Eqs. (A.1) and (A.6) in Appendix A)

$$(1+x_0^{v^*+1})(1+x_1^{v^*+1})=[\,r(v^*)\,]^2, \tag{50}$$

with

$$x_1=\frac{r(v^*)\,x_0}{1+x_0^{1+v^*}}, \tag{51}$$

and (cf. Eq. (18))

$$s(v^*)=\frac{r'(v^*)}{r(v^*)}-\left[\frac{x_0^{1+v^*}\log x_0}{1+x_0^{1+v^*}}+\frac{x_1^{1+v^*}\log x_1}{1+x_1^{1+v^*}}\right]\Big/2=0 \tag{52}$$

simultaneously for x_0, x_1 and v^*. The solution can be confirmed to be a period two ESS, if the conditions

$$s'(v^*)<0\quad\text{and}\quad|D_2|<1 \tag{53}$$

are satisfied, where

$$D_2=\frac{r(v^*)^2\,(1-v^*x_0^{1+v^*})(1-v^*x_1^{1+v^*})}{(1+x_0^{1+v^*})^2\,(1+x_1^{1+v^*})^2} \tag{54}$$

is calculated in the same way as the stability condition (16).

We used the equations above to calculate the regions in the $p-q$ plane where various types of ESS exist, for several values of r_0. For $r_0>2$ no interior ESS exists that produce either equilibrium or period two dynamics. Strategy dynamics simulations show that for $r_0>2$ only a boundary ESS $v=0$ exists that produces equilibrium dynamics. This is also true when $r_0=2$, and $p>1$. For $r_0=2$ and $p\leqslant 1$, there is still only the boundary ESS

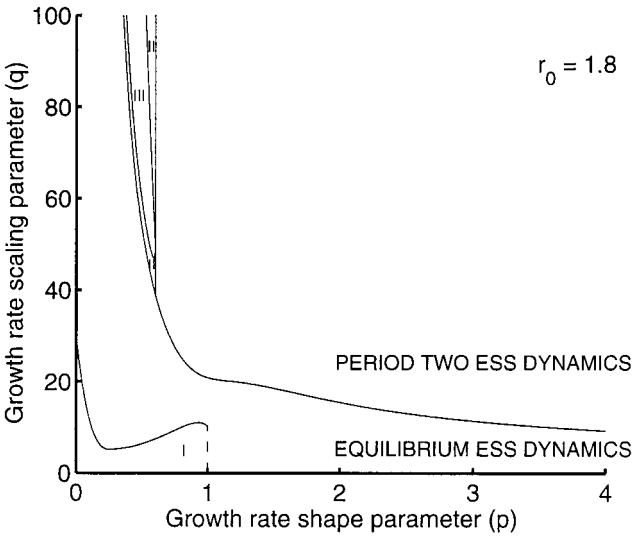

FIG. 6. Types of attractors associated with ESSs of the model (42) are plotted in $r-\gamma$ parameter space when $r_0 = 1.8$. Region I corresponds to boundary ESSs with an equilibrium density state, and the rest to interior ESSs. In region II period two ESSs can coexist with ESSs that produce more complex dynamics, and in region III the ESS attractors are more complex than period two.

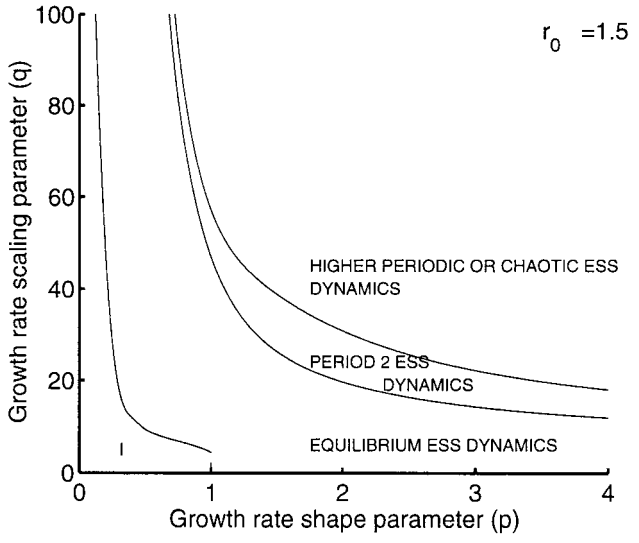

FIG. 7. Types of attractors associated with the model (42) when $r_0 = 1.5$. Region I corresponds to boundary ESSs with equilibrium density states, and the rest to interior ESSs.

$v = 0$, but for high enough values of q this could correspond to periodic or chaotic dynamics. An example is $r_0 = 2$, $p = 1$: When $q = 10$, the boundary ESS still corresponds to equilibrium dynamics, but when $q = 20$ the dynamics is period four, and when $q = 25$ it is chaotic.

When $r_0 < 2$, interior ESSs do exist, corresponding to equilibrium, periodic, or chaotic dynamics, depending on the values of p and q. (Recall that no interior ESS corresponding to equilibrium dynamics is possible in the case of the model (1), with r constant.)

The various possibilities for $r_0 = 1.8$ are shown in Fig. 6. Interior ESSs exist everywhere in the p-q plane, except in the region I, where strategy dynamics simulations indicate that a boundary ESS $v = 0$ exists, corresponding to equilibrium dynamics. In region II, ESSs corresponding to period two dynamics can coexist with ESSs corresponding to more complex dynamics (i.e., more than one ESS for the same values of p and q). In region III the only interior ESSs are those corresponding to periodic states other than period two, or chaotic states. In the remaining parts of Fig. 6, the only ESSs are those corresponding to equilibrium dynamics for lower values of q and those corresponding to period two dynamics for higher values of q. This was confirmed by strategy dynamics simulations. Recall that, in the case of the constant r model (1), $r = 1.8$ corresponded to an ESS with period two dynamics, as in the case of the present model for $r_0 = 1.8$ and high values of q.

The various types of ESSs for $r_0 = 1.5$ are shown in Fig. 7. Once again there is a region I in which only a boundary ESS with equilibrium dynamics exists. Above and to the right of this is a region of interior ESSs corresponding to equilibrium states. This region is bounded above by a curve on which $D_1 = -1$. Above this curve is a region of ESSs corresponding to period two dynamics, bounded above by a curve on which $D_2 = -1$. Strategy dynamics simulations indicate that above this region ESSs exist which correspond to higher periodic or chaotic dynamics. For example, when $r_0 = 1.5$ and $p = 2$, the upper bounds for ESSs corresponding to equilibrium and period two dynamics respectively are $q = 19.613$ and $q = 30.761$. When $q = 31$, a strategy dynamics simulation converges to a value $v^* = 7.819$, and a period four dynamics in x_t. At $q = 34$, the simulation converges to $v^* = 8.347$, and period 28 dynamics, and at $q = 35$ the ESS value of v is 8.348, and the dynamics are chaotic.

It is of interest to note, in the context of the trade-off examined above, that evolution tends to stabilize chaotic systems. Specifically, for many of the cases where p and q are chosen to be in the ESS equilibrium producing regions shown in Figs. 6 and 7, the evolutionary model (i.e., the model that combines Eq. (42) with a strategy dynamics equation for parameter v similar to the previous strategy dynamics Eq. (23) for γ) converges to an equilibrium state for a wide range of initial values of v and x_0 that correspond to chaotic dynamics for constant v. Thus, we have formulated a method for stabilizing chaotic solutions to Eq. (1). Our approach and methods of analysis are somewhat different to those

proposed by Doebeli (1995) who formulated a feedback control for a mutant invading a resident population model by Eq. (1), where the control consisted of the resident manipulating the value of its K as a function of how far both populations are from their combined equilibrium. From a biological point of view, Doebeli's approach is difficult to interpret since r and γ in Eq. (1) are primarily population parameters subject to selection while the carrying capacity parameter K is primarily an environmental parameter. Of course, the value of the parameter K may also be influenced by the characteristics of individuals in the population. In this case, however, selection acting on to underlying population characteristics to change the value of K will probably also change r or γ (cf. Getz, 1993).

5. GROWTH RATE IS A FUNCTION OF DENSITY-DEPENDENT ABRUPTNESS

Finally we extend the model (42) by allowing v (and therefore γ and r) to be density-dependent. As before, we assume a linear relationship

$$v = v(x) = ax + b, \tag{55}$$

and our model now becomes

$$x_{t+1} = \frac{r(v(x_t))\, x_t}{1 + x_t^{v(x_t)+1}}, \quad v(x_t) > 0. \tag{56}$$

In the case of an ESS corresponding to an equilibrium state, density-dependent abruptness becomes irrelevant: These ESSs are exactly the same as for the model (42) with constant v.

We used the following strategy dynamics system to investigate ESSs with more complex dynamics,

$$\begin{aligned} x_{t+1} &= \frac{r(v_t(x_t))\, x_t}{1 + x_t^{v_t(x_t)+1}} \\ a_{t+1} &= a_t + \sigma^2 \frac{\partial}{\partial a}\left[\log \left| \frac{r(v_t(x_t))}{1 + x_t^{v_t(x_t)+1}} \right| \right], \\ b_{t+1} &= b_t + \sigma^2 \frac{\partial}{\partial b}\left[\log \left| \frac{r(v_t(x_t))}{1 + x_t^{v_t(x_t)+1}} \right| \right], \end{aligned} \tag{57}$$

where $v_t(x_t) = a_t x_t + b_t$. (Note that we are allowing both density-dependent parameters to evolve, analogous to what we did in the second part of Section 3.)

Unlike the constant r, density-dependent γ model (26), strategy dynamics simulations now indicated the presence of interior ESSs with at least periodic dynamics. Thus, as a first step, we formulated the theoretical conditions for an ESS with period two dynamics and used it to map the regions in the p-q plane where such ESSs exist.

The conditions for an ESS with period two dynamics can be formulated as follows: Let $\{a^*, b^*\}$ be the ESS strategy of a resident population with corresponding period two dynamics oscillating between x_0 and x_1, and $\{a, b\}$ the slightly different strategy of a mutant population. Recalling definition (55), the invasion exponent for a resident population with a period two state $\{x_0, x_1\}$ is

$$I(r_0, p, q, a, b, x_0, x_1) = \left[\sum_{i=0}^{1} \log \left| \frac{r(v(x_i))}{1 + x_i^{1+v(x_i)}} \right| \right] \Big/ 2. \tag{58}$$

The appropriate selective differential pressures are

$$s_1(a, b) = \frac{\partial I(r_0, p, q, a, b, x_0, x_1)}{\partial a} \tag{59}$$

and

$$s_2(a, b) = \frac{\partial I(r_0, p, q, a, b, x_0, x_1)}{\partial b}. \tag{60}$$

The conditions for an interior ESS with period two dynamics are then first the conditions for a period two attractor

$$(1 + x_0^{1+v(x_0)})(1 + x_1^{1+v(x_1)}) = r(v(x_0))\, r(v(x_1)), \tag{61}$$

$$x_1 = \frac{r(v(x_0))\, x_0}{1 + x_0^{1+v(x_0)}}, \tag{62}$$

and the stability condition

$$|\bar{D}_2| < 1, \tag{63}$$

where

$$\bar{D}_2 = \prod_{i=0}^{1} \left[\frac{\partial}{\partial x} \frac{r(v(x))\, x}{1 + x^{1+v(x)}} \right]_{x = x_i}. \tag{64}$$

These are combined with the requirement that the invasion exponent should be a maximum for $a = a^*$, $b = b^*$, for which the conditions are

$$s_1(a^*, b^*) = z_2(a^*, b^*) = 0 \tag{65}$$

and

$$I_{aa}(r_0, p, q, a^*, b^*, x_0, x_0) < 0,$$
$$[(I_{ab})^2 - I_{aa}I_{bb}]_{(a,b)=(a^*,b^*)} < 0. \tag{66}$$

An interior ESS is then identified by solving (61), (62) and (65) simultaneously, and testing the solution against the restraints (63), (66) as well as

$$\min\{v(x_0), v(x_1)\} > 0. \tag{67}$$

The various possibilities for $r_0 = 1.5$ are illustrated in Fig. 8: Region I is exactly the region I of Fig. 7 for constant v, containing boundary ESSs corresponding to equilibria. The region for equilibrium state ESSs are also the same as in Fig. 7. The upper bound for interior ESSs with period two dynamics in Fig. 7 is also reproduced in Fig. 8 as a dashed curve (for purpose of comparison). Above the upper boundary curve for equilibrium state ESSs are three regions, II, III and IV. Region II is the region in which interior ESSs with period two dynamics exist. Region III contains no ESSs with period two dynamics, but strategy dynamics simulations indicate the presence of interior ESSs with more complex dynamics. From extensive simulations, using the strategy dynamics equations (57), we found only boundary ESSs with period two dynamics in the remaining region IV.

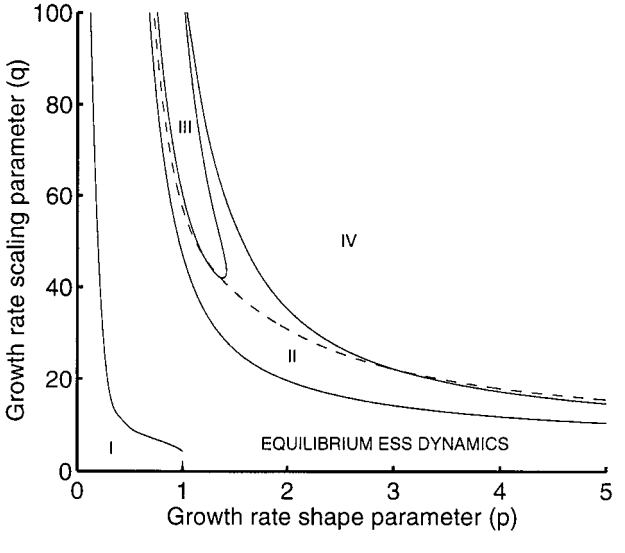

FIG. 8. Types of attractors associated with the model (56) when $r_0 = 1.5$. Region I corresponds to boundary ESSs with equilibrium density states, and IV to boundary ESSs with period two dynamics. The rest are interior ESSs, with II a region of period two density states, and III a region of more complex density states. The dashed line is the upper bound for ESSs of period 2 in Fig. 7, which we include here for purposes of comparison.

We note the following regarding the ESSs in regions II, III and IV:

1. The slope a of the ESS density-dependent abruptness is mainly negative, except when $p \leqslant 1.58$. For these values of p, ESSs in lower parts of II and III have *positive* values of a. For instance, if $p = 1.5$, $q = 30$, which is in region II, the ESS is $a^* = 1.8163$, $b^* = 7.30786$, with period two dynamics. Using the system

$$x_{t+1} = \frac{r(v)\, x_t}{1 + (x_t + y_t)^{v+1}}$$
$$y_{t+1} = \frac{r(a(x_t + y_t) + b)\, y_t}{1 + (x_t + y_t)^{a(x_t + y_t) + b + 1}} \tag{68}$$

we played this strategy against that of a resident population with constant ESS $v^* = 8.83152$. We found that competition between these strategies led to invasion of the resident. Thus, even though the ESS from the class of linear functions has a positive slope a, it is indeed a better strategy for these values of p and q than the ESS from the class of constant strategies v. The same is true for $p = 1.4$, $q = 44$, which is in region III. A strategy dynamics simulation converged to a strategy $a^* = 0.81$ and $b^* = 8.93$, corresponding to a period eight dynamics. A mutant playing this strategy is able to invade (though very slowly) a resident playing the constant v strategy of $v^* = 9.5797$ (also period eight dynamics).

2. In parts of region II above region III, for particular values of p and q, the strategy dynamics Eqs. (57) converge locally onto different candidate ESS strategies. For example, when $p = 1.4$ and $q = 47$ (this point is just above the upper bound of region III at $q = 46.436$ for $p = 1.4$ (Fig. 8)), two candidate ESSs are $a = -16.9103$, $b = 22.2749$ and $a = -2.68$, $b = 11.76$. The former corresponds to a system with period two dynamics and the latter to a system with chaotic dynamics. The former is *unable* to invade while the latter is able to invade a resident phenotype playing the constant ESS strategy $v^* = 9.55$. Note that we did not extend our analysis to playing different linear strategies against one another, by appropriately extending Eqs. (68), since this is not necessary to conclude the following. Although it appears that candidate ESSs corresponding to systems with period two dynamics exist everywhere in region II, they are sometimes merely local evolutionary stable attractors (ESAs—see Rand *et al.*, 1994) rather than global ESSs that can resist invasion from all other mutant strategies (i.e. mutant strategies that are not in the neighborhood of the resident strategy).

3. In the region IV, all the strategy dynamics simulations of Eqs. (57) were ultimately constrained by the condition $\gamma > 1$ before they could converge on an ESA. The strategies obtained by the termination condition $\gamma \leqslant 1 + \varepsilon$ (where ε was sufficiently small to obtain results to two decimal places) all corresponded to systems with period two attractors. However, some of the strategies so obtained were unable to invade the corresponding constant ESS strategy. For instance, for $p = 3$, $q = 25$, the ESS strategy among the class of constant v was $v^* = 8.54$. This is an interior ESS among this class of strategies (since the value is not determined by the constraint condition $v = 1$). For these same values of p and q, the variable v strategy $a^* = -34.56$, $b^* = 35.35$ was resistant to invasion by all other strategies $v = ax + b$, where the points (a, b) (in the a-b plane) are in the neighborhood of (a^*, b^*), as wells as to the constant ESS strategy v^*. This ESS, however, is not an interior ESS, but a boundary ESS (i.e., its computation is terminated by violation of the constraint $v > 0$). The unanticipated behavior of the system for $p = 3$ and $q = 25$, however, is that $v^* = 8.54$ is also resistant to invasion by the variable candidate ESS $v = -34.56 + 35.35$. Thus it appears that in region IV multiple ESSs exist: The particular one that becomes entrenched depends on the initial conditions of the system.

4. In the region II, for larger values of q, some ESS strategies exist that produce period two dynamics and would not invade or be invaded by the corresponding constant ESS strategies. For $p = 1.7$, this cutoff point is (up to two decimal digits) at $q = 36.95$. Thus, when $p = 1.7$ and $q = 36.94$ the candidate ESS strategy $a = -21.7651$ and $b = 25.495$, which still corresponds to period two dynamics, is able to invade the constant ESS strategy $v^* = 8.5306$. It should be noted for $p = 1.7$, however, that the constant ESS strategies v^* cease to produce systems with period two attractors at $q = 35.13$ (the point on the dashed line in Fig. 8 for this value of p). Thus, for $35.13 < q \leqslant 36.94$ ESSs producing period 2 dynamics replace ESSs producing more complex dynamics, once v is allowed to become density-dependent. In this sense density-dependent abruptness has a stabilizing effect for some values of p and q.

6. CONCLUSION

It has been known for more than 20 years that simple discrete time population models, such as Eq. (1), produce complex behavior including chaos (May, 1975; May and Oster, 1976), provided the effects of density-dependent are "sufficiently nonlinear" (in our case this amounts to $\gamma > 1$). The relationship between chaotic and evolutionary dynamics also has been investigated in some detail (for reviews see Hansen, 1992; Ferrière and Fox, 1994). These studies provide insights into conditions under which chaos can be expected to evolve or be maintained in populations. Hansen (1992), for example, concludes that: "Generally, stability is favored by selection at high densities while unstability [*sic*] is favored at low densities. As the former selection pressure tends to be stronger, it is likely that a deterministically fluctuating population with constant carrying capacity will evolve towards stability." Hansen's analysis is based on a 2-dimensional discrete-time population model that describes the population size and the frequency of an allele that distinguishes genotypes (and strategy phenotypes).

Our analysis is complementary to Hansen's in that we consider the effects of evolution in terms of the strengths of the intrinsic growth rate r and abruptness in the onset of density-dependence γ, rather than population density per se. The generalized Beverton–Holt growth model (1) is a description of a discrete generation population whose dynamics are wholly determined by a self-generating density-dependent feedback mechanism. This mechanism arises from the population exploiting an underlying resource base that is renewed each generation at a level determined by a constant set of environmental factors (that is, none of the environmental factors are dynamically linked to the population itself). Although this model is too simple to adequately capture the dynamics of populations with overlapping generations or population structures that differentially affect the response of individuals to population density, it has been shown to be a useful description for several insect populations (Bellows, 1981). It has already been demonstrated (Getz, 1996) through an ESS analysis that populations for which Eq. (1) is a useful model should evolve to promote the early onset of density-dependence if such populations have an innate capacity to more than double their population size when densities are low (i.e., $r > 2$) while the reverse should be true in relatively slow growing populations (i.e., $r < 2$). Further, this model produces chaotic solutions even when the density independent growth rate r is close to 1, although the frequency with which almost periodic solutions "break out" into chaos (cf. Fig. 2) greatly diminishes as r approaches 1.

Here we have extended this analysis to situations where the evolutionary strategies may be linear functions of the state, rather than just constants, as well as to situations where the strategy underlies and affects the values of both the "intrinsic growth" rate and the "abruptness in

TABLE V

Summary of the Values of the ESS Solution γ^* for the Different Cases Considered Here

Cases	$r > 2$	$1 < r < 2$
1. γ is constant	$\gamma^* \to 1$	No equilibrium ESS dynamics, only period two dynamics for $r > 1.6494$.
2. $\gamma = mx + c$.	$\gamma^* \to 1$	Only boundary ESS, $\gamma^*_{min} \to 1$, $\gamma^*_{max} > 1$ (e.g., $r = 1.5$, $\gamma^*_{max} = 8.59$).
3. $r = r_0/[1 + (v/q)^p]$ $\gamma = 1 + v$, v constant	$\gamma^* \to 1$	Equilibrium ESSs occur for lower values of q, so that for low to moderate values of q the dynamics stabilizes. Note that q large implies $\gamma(v) \approx$ constant.
4. $r = r_0/[1 + (v/q)^p]$, $\gamma = 1 + v$, $v = ax + b$.	$\gamma^* \to 1$	Interior equilibrium ESSs occur for low to moderate values of q and interior periodic ESSs exist for large values of q. Note that for some $p < 1.58$, the ESS value $a^* > 0$ implies γ^* is an increasing function of density. Also the ESS is no longer unique and a constant and a linear ESS can resist invasions by each other for some $\{p, q\}$. This happens for large values of q, e.g., $p = 3$, $q = 25$, but disappears for some q, e.g. $p = 1.7$, $q = 90$.

density-dependence" parameters. The main mathematical results of this paper are summarized in Table 5.

Our findings are that successful state-dependent (i.e., density-dependent) ESSs are generally those for which $\gamma(x)$ is a decreasing function of x. This result has the following biological interpretation in the context of mobile females depositing their relatively sessile young on patches of resource. Females in relatively slow growing populations (i.e., $r < 2$) should tend to over disperse their young when adult densities are low and under disperse (i.e., clump) their young when adult densities are high. In this way they postpone the immediate onset of density dependence (large γ) when densities are low but promote the early onset of density dependence (γ close to 1) when densities are high.

A third way we viewed the problem was to consider that an evolutionary trade-off exists between increasing the value of γ and increasing the value of r in model (1). The results we obtained for this case indicate that rapidly growing populations evolve so that the onset of density dependence is induced as early as possible, so long as r is a decreasing function of γ. Note that we obtained these results for a particular class of functions $r(\gamma)$, but the class is general enough to include functions with or without points of inflection in decreasing from r_0 to 0 as γ increases from 0 to ∞.

Also, in considering the trade-off between r and γ, we demonstrate that interior ESSs not only exist, but for certain choices of parameters p and q that determine the relationship $r(\gamma)$ implicit in expressions (41) and (43) the corresponding ESSs also stabilize the population. This result implies that the population evolves from a chaotic or periodic state toward an equilibrium state, and this function $r(\gamma)$ provides a more natural way to stabilize the population than the control technique proposed by Doebeli (1995).

In conclusion, the generalized Beverton–Holt model provides a biologically more plausible and dynamically richer structure for exploring how evolution may shape density dependence in biological populations than other elementary growth models (e.g., logistic, Ricker and generalized Ricker, Hassell, etc.). Here we considered evolution of density dependence in the context of constant strategies, state-dependent strategies, and strategies resulting in trade-offs between different population parameters. The results provide a foundation for exploring more complicated situations in which age-structure is important, or the population is evolving in response to selective pressures from predators or dynamic resources.

APPENDIX A

Here we explain why an ESS with period two dynamics of (1) will exist only for $1.6494 < r < 2$.

We first note that (15) is equivalent to

$$(1 + x_0^{\gamma^*})(1 + x_1^{\gamma^*}) = r^2. \tag{A.1}$$

(Just multiply the two parts of (15) together.) Now put

$$M_0 = x_0^{\gamma^*}, \quad M_1 = x_1^{\gamma^*} \tag{A.2}$$

in (A.1), as well as in (19) after multiplying the latter by γ^*. This leads to the system

$$(1 + M_0)(1 + M_1) = r^2 \tag{A.3}$$

$$\frac{M_0 \log M_0}{1 + M_0} + \frac{M_1 \log M_1}{1 + M_1} = 0, \tag{A.4}$$

which can be combined into the single nonlinear equation

$$F(M_0, r) := r^2 M_0 \log M_0 + (r^2 - 1 - M_0)(1 + M_0) \times \log\left(\frac{r^2}{1 + M_0} - 1\right) = 0. \quad \text{(A.5)}$$

Once M_0 is found by solving this equation numerically, M_1 is obtained by solving Eq. (A.3) for M_1 in terms of M_0 and r (i.e., $M_1 = r^2/(1 + M_0) - 1$), γ^* is obtained by noting from the first equation in (15) that

$$M_1 = \frac{r^{\gamma^*} M_0}{(1 + M_0)^{\gamma^*}}, \quad \text{(A.6)}$$

so that

$$\gamma^* = \frac{\log(M_0/M_1)}{\log[r/(1 + M_1)]} \quad \text{(A.7)}$$

and, finally, x_0 and x_1 are obtained from the relationships

$$x_0 = M_0^{1/\gamma^*}, \quad x_1 = M_1^{1/\gamma^*}. \quad \text{(A.8)}$$

Thus we need only investigate the existence of solutions of the nonlinear equation (A.5). Figure 9 shows the various possibilities. In this figure the graph of the function $F(M_0, r)$ in (A.5) is shown for various values of r. For $r > 2$, the graph is entirely above the horizontal axis, and there are no solutions. For $r = 2$, the graph is tangent to the horizontal axis, and there is only one solution, $M_0 = 1$. Since M_1 is then also equal to one, this is in fact an equilibrium state, and not period two. For $r < 2$ there are two solutions, of which one is always less than one, and the other greater than one, until we get the extreme case when one solution tends to the limit $M_0 = 1$, the other to the limit $M_0 = 0$. A careful study of (A.5) shows that this happens when $r^2 = 2$, or $r = \sqrt{2}$. It is also clear from (A.7) that this limit would also correspond to an infinite value of γ^*. Thus solutions of (A.5) only exist when $\sqrt{2} < r < 2$.

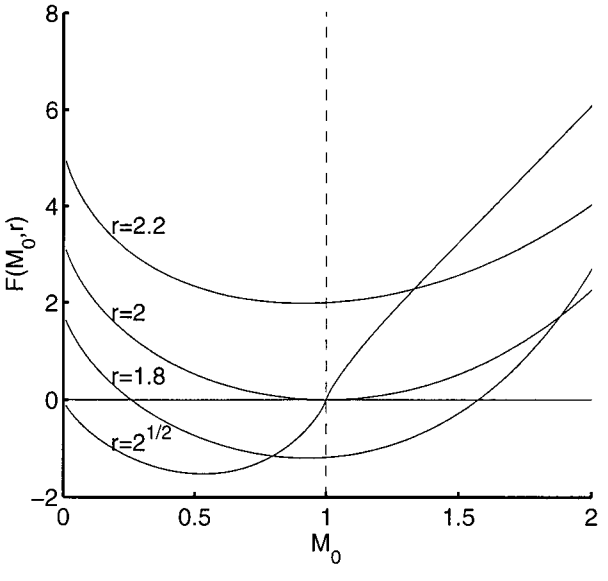

FIG. 9. Graphs of the function $F(M_0, r)$ of (A.5) for various values of r.

To qualify as an ESS, solutions of the equations above still have to satisfy the inequalities (20) and (16). The latter, when combined with (A.1), reduces to

$$|1 + (1 - \gamma^*) M_0| \, |1 + (1 - \gamma^*) M_1| < r^2. \quad \text{(A.9)}$$

The former, when combined with (A.4), reduces to

$$s'(\gamma^*) = -\frac{(\gamma^* \log M_0)^2 M_0}{2}[1 + M_0/M_1] < 0 \quad \text{(A.10)}$$

or simply

$$M_0(1 + M_0/M_1) > 0. \quad \text{(A.11)}$$

Since for $\sqrt{2} < r < 2$ either M_0 or M_1 is in the interval (0, 1), and the other larger than one, the inequality (A.11) is satisfied whenever a solution to (A.5) exists. Numerical calculations, however, show that the stability condition (A.9) is satisfied only when $r > 1.6494$. We may therefore conclude that a period two ESS will exist for $1.6494 < r < 2$.

APPENDIX B

In this Appendix we state and prove the following theorem:

THEOREM 1. *Let the mapping $R(x, u)$ be differentiable with respect to both x and u, and such that $\partial R/\partial u$ and $(1/R)(\partial R/\partial u)$ are bounded for all n-periodic points of the system*

$$x_{t+1} = R(x_t, u_t)\, x_t$$
$$u_{t+1} = u + \frac{\sigma^2}{R}\left[\frac{\partial R}{\partial u}\right]_{u = u_t,\, x = x_t}. \quad \text{(B.1)}$$

Then an attracting, n-periodic solution of the system (B.1) *is, in the limit as* $\sigma^2 \to 0$, *equivalent to an n periodic interior ESS state of the model*

$$x_{t+1} = R(x_t, u)\, x_t. \tag{B.2}$$

Moreover, if the initial values for (B.1) *are close enough to an n-periodic boundary ESS state of* (B.2), *then the sequence* $\{u_t, t = 0, 1, 2, ...\}$ *will approach that boundary for sufficiently small* σ^2.

Proof. Iterate the system (B.1) $n-1$ times, so that

$$x_{t+n} = x_t \prod_{j=0}^{n-1} R(x_{t+j}, u_{t+j}) \tag{B.3}$$

$$u_{t+n} = u_t + \sigma^2 \sum_{j=0}^{n-1} \left[\frac{1}{R} \frac{\partial R}{\partial u} \right]_{u=u_{t+j},\, x=x_{t+j}}. \tag{B.4}$$

Using the abbreviations

$$R_j = R(x_{t+j}, u_{t+j}) \quad \text{and} \quad \left(\frac{\partial R}{\partial u}\right)_j = \left(\frac{\partial R}{\partial u}\right)\Big|_{x=x_{t+j},\, u=u_{t+j}}, \tag{B.5}$$

it follows that an n-periodic solution of the system will then satisfy the conditions

$$\prod_{j=0}^{n-1} R_j = 1 \tag{B.6}$$

$$\sum_{j=0}^{n-1} \frac{1}{R_j} \left(\frac{\partial R}{\partial u}\right)_j = 0. \tag{B.7}$$

In the limit $\sigma^2 \to 0$ we may put $u_t = u_{t+1} = \cdots = u_{t+n-1} = u$ in (B.6) and (B.7), in which case (B.6) becomes the condition for an n-periodic solution of (B.2), and (B.7) the condition $s(u) = 0$ for an interior ESS with respect to u, where

$$s(u) = (1/n) \frac{\partial}{\partial u} \sum_{j=0}^{n-1} \log |R(x_{t+j}, u)|. \tag{B.8}$$

An n-periodic solution of (B.1) will be an attractor if both eigenvalues of the Jacobian matrix of the iterated system (B.4) at its corresponding fixed point are within the unit circle.

The Jacobian matrix of (B.4) is

$$J = \begin{bmatrix} J_{11} & J_{12} \\ J_{21} & J_{22} \end{bmatrix}, \tag{B.9}$$

where

$$J_{11} = \frac{\partial}{\partial x_t} \left[x_t \prod_{j=0}^{n-1} R(x_{t+j}, u_{t+j}) \right] = \frac{\partial}{\partial x_t} \left[x_t \prod_{j=0}^{n-1} R(x_{t+j}, u) \right] + O(\sigma^2), \tag{B.10}$$

$$J_{12} = x_t \frac{\partial}{\partial u_t} \prod_{j=0}^{n-1} R(x_{t+j}, u_{t+j}) = x_t \sum_{j=0}^{n-1} \prod_{\substack{k=0 \\ k \neq j}}^{n-1} R(x_{t+k}, u_{t+k}) \left(\frac{\partial R}{\partial u}\right)_j [1 + O(\sigma^2)] = x_t \left[\prod_{k=0}^{n-1} R_k \right] \left[\sum_{j=0}^{n-1} \frac{1}{R_j} \left(\frac{\partial R}{\partial u}\right)_j \right] + O(\sigma^2), \tag{B.11}$$

$$J_{21} = \sigma^2 \frac{\partial}{\partial x_t} \left[\sum_{j=0}^{n-1} \frac{1}{R_j} \left(\frac{\partial R}{\partial u}\right)_j \right], \tag{B.12}$$

$$J_{22} = 1 + \sigma^2 \frac{\partial}{\partial u_t} \left[\sum_{j=0}^{n-1} \frac{1}{R_j} \left(\frac{\partial R}{\partial u}\right)_j \right] = 1 + n s'(u_t)\, \sigma^2 + O((\sigma^2)^2). \tag{B.13}$$

Retaining only terms up to $O(\sigma^2)$, we find that the two eigenvalues of J at the n-periodic state

$$x_{t+j} = x_j, \quad u_{t+j} = u_j, \quad j = 0, 1, ..., n-1 \tag{B.14}$$

are

$$\lambda_1 = \left[\frac{\partial}{\partial x_t} \left\{ x_t \prod_{j=0}^{n-1} R(x_{t+j}, u_0) \right\} \right]_{x_t = x_0} + O(\sigma^2) \tag{B.15}$$

and

$$\lambda_2 = 1 + n\sigma^2 s'(u_0). \tag{B.16}$$

When the n-periodic solution of (B.1) is an attractor, $|\lambda_1| < 1$ and $|\lambda_2| < 1$. In the limit $\sigma^2 \to 0$ this corresponds to the two conditions

$$\left| \left[\frac{\partial}{\partial x_t} \left\{ x_t \prod_{j=0}^{n-1} R(x_{t+j}, u_0) \right\} \right]_{x_t = x_0} \right| < 1 \tag{B.17}$$

and

$$s'(u_0) < 0. \tag{B.18}$$

The first is exactly the condition for an n-periodic solution of (B.2) to be an attractor, and the second, together with the equation $s(u_0) = 0$ which we already showed

to be valid in this limit, are the conditions for the appropriate invasion exponent to be a maximum. Thus an attracting n-periodic solution of (B.1) implies a n-periodic state interior ESS of (B.2) with respect to the strategy u. The converse is easily seen to be true as well, which proves equivalence.

When (B.2) has a boundary ESS at the left (right) boundary, $s(u) < 0$ (> 0) when u is sufficiently near to that boundary. Since the second equation of the iterated system (B.4) can be written in the form

$$u_{t+n} = u_t + n\sigma^2(u_t) + O((\sigma^2)^2), \qquad \text{(B.19)}$$

u_t would move nearer to the boundary after each cycle of n iterations, provided that σ^2 is small enough for the $O((\sigma^2)^2)$ term to be negligible. ∎

Simulations shows that the system (B.1) will also converge to an interior ESS, or move towards a boundary ESS in case of chaotic state ESSs. A heuristic explanation for this is the following: For large n, the term

$$\sigma^2 \sum_{j=0}^{n-1} \left[\frac{1}{R} \frac{\partial R}{\partial u} \right]_{u = u_{t+j},\, x = x_{t+j}}$$

in the second equation of the system (B.4) is at least proportional to an approximation of the selective differential pressure $s(u)$ of the chaotic attractor, in the sense that it would have the same sign as $s(u)$, and be near to zero when $s(u) = 0$. Thus u_t would evolve towards an ESS, and x_t would converge to the corresponding (chaotic) attractor.

REFERENCES

Bellows, T. S. 1981. The descriptive properties of some models for density dependence, *J. Animal Ecol.* **50**, 139–156.

Doebeli, M. 1995. Updating Gillespie with controlled chaos, *Am. Nat.* **146**, (3), 479–487.

Ellis, E., Jr., Johnson, E. W., Lodi, E., and Schwalbe, D. 1992. "Maple V Flight Manual," Brooks/Cole, Pacific Grove, Ca.

Ferrière, R., and Fox, A. G. 1995. Chaos and evolution, *TREE* **10**, (12), 480–485.

Ferrière, R., and Gatto, M. 1995. Lyaponov exponents and the mathematics of invasion in oscillatory or chaotic populations, *Theor. Popul. Biol.* **48**, 126–171.

Gage, M. J. G. 1995. Continuous variation in reproductive strategy as and adaptive response to population density in the moth, *Plodia interpunctella*, *Proc. R. Soc. London B* **261**, 25–30.

Getz, W. M. 1993. Metaphysiological and evolutionary dynamics of populations exploiting constant and interactive resources: $r - K$ selection revisited, *Evol. Ecol.* **7**, 287–305.

Getz, W. M. 1996. A hypothesis regarding the abruptness of density dependence and the growth rate of populations, *Ecology* **77**, 2014–2026.

Getz, W. M., and Kaitala, V. 1989. Ecogenetic models, competition, and heteropatry, *Theor. Popul. Biol.* **36**, 34–58.

Getz, W. M., and Kaitala, V. 1993. Ecogenetic analysis and evolutionary stable strategies in harvested populations, *in* "The Exploitation of Evolving Resources" (K. Stokes, J. McGlade, and, R. Law, Eds.), pp. 187–203, Springer-Verlag, Berlin.

Guisande, C. 1993. Reproductive strategy as population density varies in *Daphnia magna* (*Cladocera*), *Freshwater Biol.* **29**, 463–467.

Hansen, T. F. 1992. Evolution of stability parameters in single-species population models: Stability or chaos, *Theor. Popul. Biol.* **42**, 199–217.

Kaitala, A., Kaitala, V., and Lundberg, P. 1993. A theory of partial migration, *Am. Nat.* **142**, 59–81.

Kaitala, V., Kaitala, A., and Getz, W. M. 1989. Evolutionary stable dispersal of a waterstrider in a temporally and spatially heterogeneous environment, *Evol. Ecol.* **3**, 283–298.

Kaitala, V., Mappes, T., and Ylönen, H. 1997. Delay female reproduction in equilibrium and chaotic populations, *Evol. Ecol.* **11**, 105–126.

May, R. M. 1974. Biological populations with nonoverlapping generations: Stable points, stable cycles, and chaos, *Science* **186**, 645–647.

May, R. 1975. Biological populations obeying difference equations: Stable points, stable cycles, and chaos, *J. Theor. Biol.* **51**, 511–524.

May, R. M., and Oster, G. F. 1976. Bifurcations and dynamic complexity in simple ecological models, *Am. Nat.* **110**, 573–590.

Maynard-Smith, J. 1973. "Models in Ecology," Cambridge Univ. Press, Cambridge, UK.

Maynard-Smith, J., and Slatkin, M. 1973. The stability of predator-prey system, *Ecology* **54**, 384–391.

Rand, D. A., Wilson, H. B., and McGlade, J. M. 1994. Dynamics and evolution: Evolutionary stable attractors, invasion exponents and phenotype dynamics, *Philos. Trans. R. Soc. London* **343**, 261–283.

Shepherd, J. G. 1982. A versatile new stock-recruitment relationship for fisheries, and the construction of sustainable yield curves, *J. Cons. Int. Explor. Mer.* **40**, 67–75.

Sober, E. 1984. "The Nature of Selection," Univ. of Chicago Press, Chicago.

Vincent, T. L. 1990. "Dynamics of Complex Interconnected Biological Systems," Birkhauser, Boston.

Vincent, T. L., Cohen, Y., and Brown, J. S. 1993. Evolution via strategy dynamics, *Theor. Popul. Biol.* **44**, 149–176.

Vincent, T. L., and Fisher, M. E. 1988. Evolutionary stable strategies in differential and difference models, *Evol. Ecol.* **2**, 321–337.

Vincent, T. L., Van, M. V., and Goh, B. S. 1996. Ecological stability, evolutionary stability, and the ESS maximum principle, *Evol. Ecol.* **10**, 567–591.

Yasuda, H. 1990. Effect of population density on reproduction of two sympatric dung beetle species *Aphodius harodianu* and *A. elegans* (Coleoptera: Scarabaeidea), *Res. Popul. Ecol.* **32**, 99–111.